Laboratory examinations were normal including blood NH_3, blood gas analysis, serum lactate, blood glucose, cerebrospinal fluid (CSF) glucose, CSF lactate, CSF white cell count, blood amino acid analysis, urine organic acid analysis, and plasma very long-chain fatty acid (VLCFA). Chromosome analysis and fluorescent in situ hybridization (FISH) studies for the LIS1 specific deletion at 17p13.3 revealed no abnormalities.

Her electroencephalogram (EEG) showed low amplitude and irregular waking background without obvious epileptic discharges on day 0. The ictal EEG of complex partial seizures at 3 months of age revealed right fronto-central spike bursts. Auditory evoked potentials (ABRs) and visual evoked potentials (VEPs) both showed a flat pattern. Brain magnetic resonance imaging (MRI) on day 0 revealed hypoplasia of bilateral cerebral hemispheres with enlarged extraaxial space, a simplified gyral pattern without a thickened cortex, a relatively spared volume of the bilateral basal ganglia and thalamus, a mildly flattened brain stem, and a hypoplastic corpus callosum (**Fig. 1a–c**).

Patient 2

The microcephaly of the younger sister was recognized at a gestational age (GA) of 28 weeks by means of ultrasonography. She was born after 37 weeks gestation by spontaneous delivery following a normal pregnancy. The patient's birth weight was 2566 g (−0.5 SD), length 46.0 cm (−0.7 SD), and OFC 27 cm (−4.0 SD). Her Apgar score was 8 at 1 min, and 9 at 5 min. She developed generalized tonic seizures at 3 months of age. Her seizures were well controlled with valproic acid beginning when she was 2 years old.

She was able to bottle feed through the first 12 months, but her feeding skills deteriorated beginning at 18 months of age. At 2 years and 6 months, she was also diagnosed with GERD and required the use of a duodenal feeding tube. She also had spastic quadriplegia and visual impairment from early infancy. No developmental progress was observed.

Clinical examination performed at 3 years and 1 month of age showed microcephaly of OFC 41.5 cm (−4.2 SD), and other growth parameters were between −1 and −2 SD. Her dysmorphism was similar to that of her older sister. She had marked scoliosis, with hypertonic extremities and a posture characterized by asymmetrical tonic neck reflex. Deep tendon reflexes were exaggerated, and ankle clonus appeared bilaterally. Erratic myoclonus in the bilateral orbicular muscles and systemic myoclonus easily induced by sounds were often seen. There was no spontaneous movement of the extremities.

Laboratory examinations were normal including blood chemistry, creatinine kinase, intrauterine infection screen, blood NH_3, blood gas analysis, serum lactate, serum glucose, CSF glucose, CSF lactate, CSF white cell count, blood amino acid analysis, urine organic acid analysis, and plasma VLCFA. Chromosome analysis (G band) was 46XX; FISH for the LIS1 specific deletion at 17p13.3 was negative. Array-based comparative genomic hybridization (array-CGH) was performed using the Agilent Human Genome Microarray kit 244A (Agilent Technologies, Santa Clara, CA, USA), and it showed no apparent deletions or duplication.

The brain MRIs were performed at a GA of 30 weeks via intrauterine imaging, at day 0, and at 3 years and 1 month (**Fig. 2a–g**). The former 2 MRI findings were almost identical to those of the older sister. Cerebellar white matter around the dentate nucleus had high T_2 signal intensity, showing unmyelinated cerebellar white matter. The MRI at 3 years and 1 month of age demonstrated marked dilatation of the posterior and inferior horns of the lateral ventricles and severe volume reduction of whole hemispheric gray and white matter, which was most dominant in the frontal lobes, whereas the volumes of bilateral basal ganglia, thalamus, and infratentorial structures were relatively preserved. The patient's EEG at 4 months of age and 3 years and 1 month of age demonstrated almost continuous spikes in the mid-frontal to right frontal regions. ABR and VEP were normal.

Discussion

There have been only 3 reports describing patients with microcephaly with simplified gyri and enlarged extraaxial space [1, 2, 8]. None of these reports included repeat MRI studies. As in the previous reports, our patients suggested an autosomal recessive trait of inheritance. Alternatively, an autosomal dominant or X-linked dominant inheritance with gonadal mosaisism is also possible. The genes responsible for microcephaly with simplified gyri only have been identified as *MCPH1, ASPM, CDK5RAP2, CENPJ,* and *WDR62* [1, 9]. However, it is not clear whether microcephaly with simplified gyri and enlarged extraaxial space with this phenotypic presentation can be explained by different mutation patterns of the already identified genes or whether it represents a distinct disease entity caused by still unknown genes. The extraaxial space enlargement described previously was less severe as compared to the present cases [1]. Dysmorphic features as observed in the present patients have not been described previously, although multiple anomalies, eye defects and jejunal atresia have been reported in patients with microcephaly with simplified gyri [1]. It remains to be clarified whether those phenotypic and neuroradiological features suggest distinctive clinical entity. Moreover, there may be overlap in the MRI findings between patients with microcephaly with simplified gyri and enlarged extraaxial space and those with microcephaly with simplified gyri and both enlarged extraaxial space

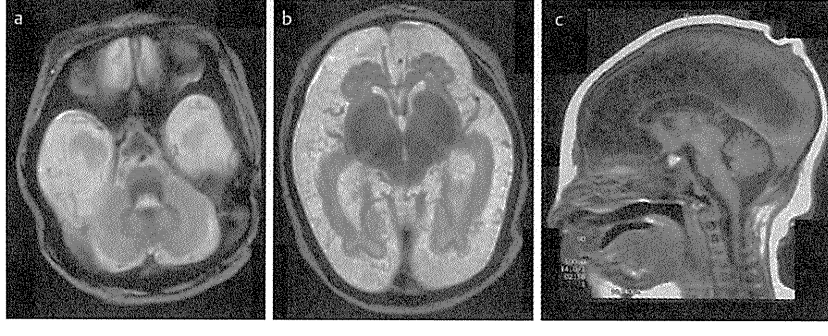

Fig. 1 Brain MRI of older sister at age of day 0. The MRI (**a** and **b**: T_2-weighted image [TR 4000, TE 132], **c**: T_1-weighted image [TR 500, TE 14.0]) showing hypoplasia of bilateral cerebral hemispheres with enlarged extraaxial space, a simplified gyral pattern without a thickened cortex, hypoplastic corpus callosum, and a mildly flattened brain stem.

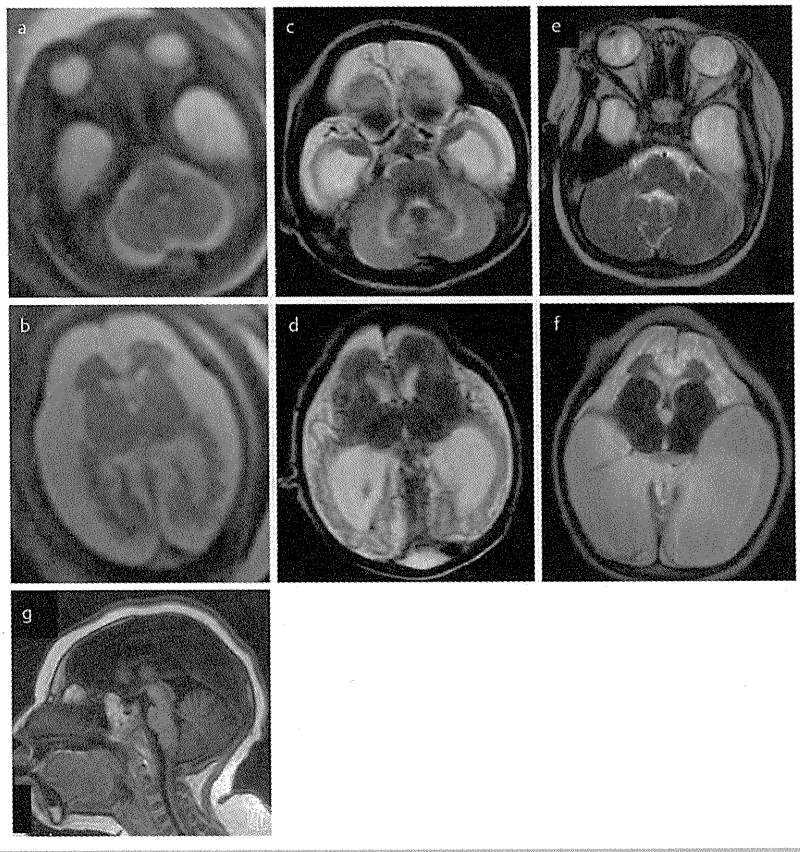

Fig. 2 Brain MRI with T_2-weighted images [TR 4500, TE 90] (**a–f**) and T_1-weighted images [TR 500, TE 14.0] (**g**) of the younger sister at 30 weeks gestational age (**a**, **b**), day 0 (**c**, **d**), and 3 years and 1 month of age (**e–g**). The MRI at 30 weeks gestational age and day 0 (**a–d**) revealed hypoplasia of bilateral cerebral hemispheres, particularly in the frontal regions, with enlarged extraaxial space, a simplified gyral pattern without thickened cortex, and enlarged lateral ventricles, especially in the posterior and temporal horns, with a reduction in the surrounding white matter. There was no change in the findings between GA 30 weeks and day 0. High signal intensity was observed in the lateral sides of the dentate nucleus (**c**). The MRI at 3 years and 1 month of age (**e–g**) demonstrated progressive dilatation of the posterior and inferior horns of the lateral ventricles, with a volume reduction in the surrounding hemispheric structures, especially in the frontal lobe. Some extent of myelination in the cerebellar hemisphere was observed (**e**). The size of the basal ganglia and thalamus, as well as of the infratentorial structures, was relatively preserved (**g**).

and pontocerebeller hypoplasia, because the older sister in our study had a mildly flattened brain stem at age of day 0. On the other hand, pontocerebeller hypoplasia may be the result of extensive cerebral pathology, as seen in the pontocerebeller hypoplasia in preterm infants [7].

A striking finding in these patients was progressive atrophy of the cerebral gray and white matter, with enlarged lateral ventricles, which was evident in the younger sister. Neurodegenerative processes such as accelerated apoptosis may be estimated from the MRI findings described in this report and the clinical deterioration observed in the younger sister. Basel-Vanagaite and Dobyns also described a rapid decrease in OFC postnatally in the subgroup of patients without congenital microcephaly but with enlarged extraaxial space [1]. Similar progressive changes in the cerebrum have also been reported in a patient most likely categorized as microcephaly with simplified gyri and pontocerebeller hypoplasia [4].

In spite of remarkable volume reductions in cerebral hemisphere cortices and white matter, the size of the bilateral basal ganglia, thalamus, and infratentorial structures was relatively preserved in these cases. As a cortical ribbon was formed and periventricular nodular heterotopia or band heterotopia was not observed, migration of cortical neurons from the ventricular zone may not be involved, but the proliferation process of neuronal and glial cells in the ventricular zone may be altered. On the other hand, the proliferation of neuronal cells in the lateral ganglionic eminence that generates the striatum and in the medial ganglionic eminence that mostly generates the globus pallidus and septum [3, 6] may not be involved, although tangential migration of cortical GABAergic interneurons from the ganglionic eminence may have been altered [5].

In conclusion, it is believed that the genes responsible for microcephaly with simplified gyri and enlarged extraaxial space are involved in the neuronal and glial proliferation in the ventricular zone as well as in tangiential neuronal migration. Moreover, the nature of progressive degeneration of the hemispheric structures should be clarified in the near future.

Affiliations

[1]Department of Pediatrics, Tohoku University School of Medicine, Sendai, Japan
[2]Department of Pediatric Neurology, Takuto Rehabilitation Center for Children, Sendai, Japan
[3]Department of Nursing, Yamagata University Faculty of Medicine, Yamagata, Japan
[4]Ishinomaki Red Cross Hospital, Ishinomaki, Japan
[5]Department of Pediatrics, Yamagata University Faculty of Medicine, Yamagata, Japan
[6]Tokyo Women's Medical University Institute for Integrated Medical Sciences, Tokyo, Japan

References

1 *Basel-Vanagaite L, Dobyns WB.* Clinical and brain imaging heterogeneity of severe microcephaly. Pediatr Neurol 2010; 43: 7–16
2 *Basel-Vanagaite L, Marcus N, Klinger G et al.* New syndrome of simplified gyral pattern, micromelia, dysmorphic features and early death. Am J Med Genet A 2003; 119: 200–206
3 *Deacon TW, Pakzaban P, Isacson O.* The lateral ganglionic eminence is the origin of cells committed to striatal phenotypes: neural transplantation and developmental evidence. Brain Res 1994; 668: 211–219
4 *Kure-Kageyama H, Saito Y, Maegaki Y et al.* A patient with simplified gyral pattern followed by progressive brain atrophy. Brain Dev 2007; 29: 383–386
5 *Letinic K, Zoncu R, Rakic P.* Origin of GABAergic neurons in the human neocortex. Nature 2002; 417: 645–649

6 *Olsson M, Campbell K, Wictorin K et al.* Projection neurons in fetal striatal transplants are predominantly derived from the lateral ganglionic eminence. Neuroscience 1995; 69: 1169–1182
7 *Srinivasan L, Allsop J, Counsell SJ et al.* Smaller cerebellar volumes in very preterm infants at term-equivalent age are associated with the presence of supratentorial lesions. AJNR Am J Neuroradiol 2006; 27: 573–579
8 *Woods CG, Bond J, Enard W.* Autosomal recessive primary microcephaly (MCPH): a review of clinical, molecular, and evolutionary findings. Am J Hum Genet 2005; 76: 717–728
9 *Yu TW, Mochida GH, Tischfield DJ et al.* Mutations in WDR62, encoding a centrosome-associated protein, cause microcephaly with simplified gyri and abnormal cortical architecture. Nat Genet 2010; 42: 1015–1020

Comparison of Three Methods for Localizing Interictal Epileptiform Discharges With Magnetoencephalography

Hideaki Shiraishi,† Seppo P. Ahlfors,*‡ Steven M. Stufflebeam,*‡ Susanne Knake,*§ Pål G. Larsson,‖ Matti S. Hämäläinen,*‡ Kyoko Takano,† Maki Okajima,† Keisaku Hatanaka,¶ Shinji Saitoh,† Anders M. Dale,*# and Eric Halgren*#*

Purpose: To compare three methods of localizing the source of epileptiform activity recorded with magnetoencephalography: equivalent current dipole, minimum current estimate, and dynamic statistical parametric mapping (dSPM), and to evaluate the solutions by comparison with clinical symptoms and other electrophysiological and neuroradiological findings.

Methods: Fourteen children of 3 to 15 years were studied. Magnetoencephalography was collected with a whole-head 204-channel helmet-shaped sensor array. We calculated equivalent current dipoles and made minimum current estimate and dSPM movies to estimate the cortical distribution of interictal epileptiform discharges in these patients.

Results: The results for four patients with localization-related epilepsy and one patient with Landau–Kleffner Syndrome were consistent among all the three analysis methods. In the rest of the patients, minimum current estimate and dSPM suggested multifocal or widespread activity; in these patients, the equivalent current dipole results were so scattered that interpretation of the results was not possible. For 9 patients with localization-related epilepsy and generalized epilepsy, the epileptiform discharges were wide spread or only slow waves, but dSPM suggested a possible propagation path of the interictal epileptiform discharges.

Conclusion: Minimum current estimate and dSPM could identify the propagation of epileptiform activity with high temporal resolution. The results of dSPM were more stable because the solutions were less sensitive to background brain activity.

Key Words: MEG, epilepsy, dynamic statistical parametric mapping, minimum current estimate, minimum norm estimate, equivalent current dipole.

(*J Clin Neurophysiol* 2011;0: 1–10)

In addition to seizures, the spontaneous activity of epileptogenic tissue is characterized by interictal epileptiform discharges (IEDs), consisting of spikes, sharp waves, and slow waves (Pedley, 1984; Penfield and Jasper, 1954). There are usually thousands of IEDs to each seizure; thus, IEDs are easier to record than ictal discharges (IDs). Patients with focal medically refractory epilepsies may have the chance to undergo epilepsy surgery. In those patients, a comprehensive and careful presurgical evaluation including an estimate of the seizure onset zone and the irritative zone generating the IED is crucial (Doherty and Cole, 2001; Ebersole and Pacia, 1996; Rosenow and Lüders, 2001). The use of IEDs in predicting the epileptogenic focus and in defining the surgical target is becoming better appreciated and may become increasingly useful as the physiologic relation of ictal and interictal discharges becomes better understood (Baumgartner et al., 1995; Blume, 2001; Cascino et al., 1996; Cendes et al., 2000). A correct identification of the irritative zone by EEG recordings contributes to the definition of the epilepsy syndrome and to planning of a resective procedure or of invasive studies using subdural or depth electrodes when noninvasive studies remain inconclusive or discordant (Knake et al., 2006).

To localize the surgical target, seizure semiology and information from multiple techniques, including magnetoencephalography (MEG), EEG, MRI, single photon emission computed tomography, and positron emission tomography (Adelson et al., 1995; Danielpour and Peacock, 2000; Duchowny et al., 2000; Madsen et al., 1995; Nordli, 2000), are commonly compared for concordance (Spencer, 1994; Spencer and Bautista, 2000). Magnetoencephalography and EEG can provide valuable measures of normal and abnormal electrical activity in the brain (Humphrey, 1968; Nunez, 1981). Determining the extracranial magnetic fields and scalp potentials generated by a given source, known as the forward problem, is relatively well understood, and efficient and accurate algorithms are available (Hämäläinen and Sarvas, 1989; Liu et al., 2002; Oostendorp and van Oosterom, 1989). However, in general, there is no unique solution to the inverse problem of estimating the source currents based on the MEG and EEG recordings, that is, it is not possible to fully determine the pattern of sources from external measurements (Baillet et al., 2001; Dale and Sereno, 1993; Hämäläinen et al., 1993).

Early attempts to localize the source currents were based on topographic maps of the scalp potential or its spatial derivatives. The spatial spread of the scalp potential is wide, even when the underlying source is a focal one. Hjorth source derivative (also known as scalp current density or Laplacian) (Hjorth, 1970) improves this situation by tightening the topographic pattern near the source. A similar effect is obtained by estimating the potential at the brain surface (Gevins et al., 1994).

The most popular source model is the equivalent current dipole (ECD) (Hämäläinen et al., 1993; Scherg, 1992). If the true pattern of activity consists of only one or a few focal sources, they can be modeled with ECDs; the locations and dipole moments are determined

From the *MGH/MIT/HMS Athinoula A. Martinos Center for Biomedical Imaging, Massachusetts General Hospital, Harvard Medical School, Charlestown, Massachusetts, U.S.A.; †Department of Pediatrics, Hokkaido University Graduate School of Medicine, Sapporo, Japan; ‡Harvard-MIT Division of Health Sciences and Technology, Cambridge, Massachusetts, U.S.A.; §Epilepsy Center Marburg, Department of Neurology, Philipps-University, Marburg, Germany; ‖Department of Neurosurgery, Oslo University Hospital, Oslo, Norway; ¶Department of Applied Physics, Okayama University of Science, Okayama, Japan; and #Department of Radiology, University of California, San Diego, San Diego, California, U.S.A.

This study was supported by the National Institutes of Health (NS18741), the MIND Institute (DOE grant DE-FG03-99ER62764), and the National Center for Research Resources (P41RR14075).

Address correspondence and reprint requests to Hideaki Shiraishi, MD, PhD, Department of Pediatrics, Hokkaido University, Graduate School of Medicine, North 15, West 7, Kita-ku, Sapporo, 060-8638, Japan; e-mail: siraisi@nmr.mgh.harvard.edu.

ISSN: 0736-0258/11/0000-0001

AQ : 1

using parameter optimization techniques. The ECD model may fail to give meaningful results; however, if the underlying assumption about focality is not valid (Ossenblok et al., 1999). The problem of determining the locations of multiple simultaneous dipoles becomes prohibitively difficult when the number of dipoles increases. Good results have been obtained with spatiotemporal dipole modeling (Scherg, 1992; Scherg et al., 1999), in which the locations of a relatively few dipoles are assumed not to change over the analysis period. Typically, however, multidipole modeling is a tedious and time-consuming process and to some extent gives results that depend on the experience of the person analyzing the data.

In the present study, we explored the use of two source estimation methods based on the distributed source models: minimum current estimate (MCE) (Uutela et al., 1999) and dynamic statistical parametric mapping (dSPM) (Dale et al., 2000), in patients with different epilepsy syndromes. In the distributed models, the sources are not restricted to a small number of focal sources. Instead, the brain is partitioned into a large number of small patches, each represented by a current dipole, approximating any arbitrary spatial distribution of cortical activity. Because the number of sensors is typically less than the number of unknown dipole amplitudes, additional prior assumptions are made about the properties of the sources. The dSPM is based on the minimum-L2 norm estimate, minimizing the square sum of the dipole element amplitudes (Hämäläinen and Ilmoniemi, 1994), whereas the MCE is a minimum-L1 norm estimate, which minimizes the sum of absolute values of source amplitudes (Matsuura and Okabe, 1997). These approaches result in spatiotemporal maps (or movies) of brain activity with time resolution in milliseconds (Liu et al., 1998). In dSPM, a further step of normalizing the spatiotemporal estimates for noise sensitivity yields dynamic statistical parametric maps of brain activity (Dale et al., 2000). Besides decisions about prior assumptions, the methods based on distributed source models require little interference from the person analyzing the data.

We compared dSPM, MCE, and a single-ECD analysis of IEDs in MEG from a clinical viewpoint. In particular, we evaluated whether the methods give concordant localization results in patients whose clinical symptoms suggest a focal abnormality. Hence, we examined the concordance between seizure semiology and/or MRI findings, and MEG findings obtained by ECD, MCE, and dSPM analyses. Furthermore, we studied the suitability and usefulness of the distributed models for identifying widespread activity or multiple simultaneous foci. We also examined whether these models can be used to determine the sequence of propagation of epileptic activity.

PATIENTS AND METHODS

Patients

We studied 14 patients with different epilepsy syndromes who were treated at the Department of Pediatrics in the Hokkaido [T1] University Hospital (Table 1). The patients (eight boys and six girls) were 3 to 15 years old (mean, 8.9 year) at the time of recording. We classified the epilepsies and epileptic syndromes of these patients according to the criteria of the International League Against Epilepsy (Commission on Classification and Terminology of the International League Against Epilepsy, 1989). Eight patients with symptomatic localization–related epilepsy (SLRE), two patients with idiopathic localization–related epilepsy, two patients with symptomatic generalized epilepsy, a patient with idiopathic generalized epilepsy, and a patient with undetermined epilepsy were included in the present study. Among the patients with SLRE, there were four patients with frontal lobe epilepsy, a patient with temporal lobe epilepsy, and a patient with parietal lobe epilepsy. The localization of epileptogenic zone in two patients with SLRE could not be further specified. Among the patients with idiopathic localization–related epilepsy, a patient was with benign partial epilepsy with centrotemporal spikes and a patient was with atypical benign partial epilepsy in infancy with hemiconvulsive seizures and complex partial seizures accompanied by atonic seizures (Aicardi and Chevrie, 1982). One of the patients with symptomatic generalized epilepsy had Lennox–Gastaut syndrome (Gastaut et al., 1966). The patient with undetermined epilepsy had Landau–Kleffner syndrome (Landau and Kleffner, 1957).

The ECD and dSPM results of three of the present patients were also discussed in two previous reports: Patients 6 and 9 were presented in Shiraishi et al. (2005*a*) (their cases 1 and 2) as an example of the applicability of MEG to patients with epilepsy with widespread spike and slow wave activity, and patients 2 and 6 were included in Shiraishi et al. (2005*b*) (their cases 1 and 2). Here, we present the additional new results of MCE analysis on these patients.

Magnetoencephalography, EEG, and MRI Acquisition

The subjects' parents or guardians gave their written informed consent for the MEG studies. The study was approved by the local institutional review board. The MEG and EEG recordings were made in a magnetically shielded room at the Hokkaido University Hospital. Magnetoencephalography was recorded using a system with 204 superconducting quantum interference devices (Vectorview; Elekta-Neuromag, Ltd, Helsinki, Finland.). This instrument has 204 planar gradiometers arranged in orthogonal pairs in a helmet-shaped array covering the entire scalp. These types of sensors detect the maximum signal right above the source current. The MEG data were band pass filtered between 0.03 and 133 Hz and sampled at 400 Hz. EEG was recorded simultaneously for visual screening using 20 scalp electrodes, placed according to the international 10-20 system, with 2 additional electrodes for ECG monitoring. The EEG high-pass filtering time constant was 0.3 seconds. We usually recorded for a duration of >1 hour for each patient, collecting data in 4-minute blocks. The patients were in a prone position. Sedative agent was used for child patients. The relative position of the head and the MEG sensors were determined by attaching 3 small head-position indicator coils to the head. The position of the coils was digitized and subsequently recorded by the MEG sensors for coregistration with MRI (Hämäläinen et al., 1993).

High-resolution MRIs were acquired with a 1.5 T scanner (Magnetom VISION; Siemens AG, Erlangen, Germany) for diagnostic purposes and for supporting the analysis and interpretation of the MEG data (TE = 60, TR = 100 milliseconds, voxel size = $1.5 \times 1.5 \times 1.5$ mm^3).

Magnetoencephalography Source Analysis

The distribution of the brain activity generating the spikes was determined using three source estimation approaches: ECD, MCE, and dSPM. The ECD is a good model when the underlying activity is focal, that is, restricted to a relatively small region in the brain. For nonfocal activity, distributed source models such as the MCE and the dSPM are expected to be better suited than the ECD model. Equivalent current dipole and MCE solutions were computed using "xfit" and "MCE" software, respectively, from Elekta-Neuromag Ltd. The dSPM analysis was performed with in-house software (Dale et al., 2000).

AQ : 6

TABLE 1. Clinical profiles, ECD, MCE, and dSPM Findings of the 14 Patients

Case	Age	Sex	Classification	Syndrome	Seizure Types	EEG	MRI	Assumed Foci	ECD (Category*)	MCE (Category*)	dSPM (Category*)
Patients with localized spikes											
1	5	M	SLRE	FLE	FMS, HC	L F-C, CSWS	NF	LF	L F (1)	L F (1)	L F (1)
2	7	M	SLRE	FLE	FMS	Cz	NF	RF	R F (1)	R F (1)	R F (1)
3	15	M	SLRE	TLE	SPS, SCPS	LT	B MTS	LT	LT, HP (1)	LT (1)	LT, INS (1)
4	8	F	ILRE	BECT	pGTC	R T-O	NF	RF	RF (1)	RF (1)	RF (1)
5	8	F	UDE	LKS	HC	L C-F, CSWS	NF	LT, LF	LT, LF (1)	LT, LF (1)	LT, LF (1)
Patients with diffuse spikes											
6	3	M	SLRE	PLE	SPS, HC, pGTC	L FSL	NF	Left hemispheric	Scattered (3)	LP (2)	LP, LF, LP (1)
7	10	M	SLRE	FLE	CPS	B DSP	NF	Left hemispheric	LF (2)	LF (1)	LF (1)
8	13	F	SLRE	FU	SPS, pGTC	L DSP	NF	Left hemispheric	Scattered (3)	LF (2)	LF, LP, RF (1)
9	13	F	SLRE	FLE	CPS	L Fp-F	LF OS (PNET)	LF, LT	LF (2)	LF (2)	LF, LT (1)
10	8	M	SLRE	FU	SPS, SCPS	B DSL	L OP tuber (TS)	Multiple focus	R OP broad (3)	RP (2)	RF (1)
11	4	F	ILRE	ABPE	HC, CPS	L C-P, CSWS	NF	Left hemispheric	LF, LT (3)	LF, LP (2)	LF, LP (1)
Patients with generalized epilepsy											
12	14	F	SGE	Others	ToS	B DSP	NF	Bilateral diffuse	Scattered (3)	LF (2)	LF (2)
13	14	M	SGE	LGS	ToS, AABS	B DSP, DSW	B OP gliosis	Bilateral diffuse	Scattered (3)	B F broad (2)	BF, BT broad (1)
14	3	M	IGE	Others	ABS, MS, GTCS	B DSL	NF	Bilateral diffuse	Scattered (3)	B F broad (2)	B F broad (2)

*Category: (1) MEG results concordant with clinical hypothesis; (2) MEG results ipsilateral to clinical hypothesis, but different area; (3) MEG results discordant with clinical hypothesis.

AABS, atypical absence seizure; ABPE, atypical benign partial epilepsy in infancy; ABS, absence seizure; BECT, benign partial epilepsy with centrotemporal spikes; C, central; CPS, complex partial seizure; CSWS, continuous spikes and waves during sleep; DSL, diffuse slow wave; DSP, diffuse spike; DSW, diffuse spikes and slow waves; F, frontal; FLE, frontal lobe epilepsy; FMS, focal motor seizure; FSL, focal slow wave; FU, focus unknown; GTCS, generalized tonic–clonic seizure; HC, hemiconvulsive seizure; HP, hippocampus; IGE, idiopathic generalized epilepsy; ILRE, idiopathic localization–related epilepsy; INS, insular cortex; L, left; LGS, Lennox–Gastaut syndrome; LKS, Landau-Kleffner syndrome; MS, myoclonic seizure; MTS, medial temporal sclerosis; NF, no finding; O, occipital; OS, operation scar; P, parietal region; pGTC, partial seizure evolved to generalized tonic-clonic seizure; PLE, parietal lobe epilepsy; PNET, primitive neuroectodermal tumor; R, right; SCPS, simple partial seizure evolved to complex partial seizure; SGE, symptomatic generalized epilepsy; SPS, simple partial seizure; T, temporal; TLE, temporal lobe epilepsy; ToS, tonic seizure; TS, tuberous sclerosis; UDE, undetermined epilepsy.

The conductivity geometry of the head was assumed spherically symmetric in the ECD analysis, whereas a boundary element model for the head (Hämäläinen and Sarvas, 1989; Oostendorp and van Oosterom, 1989) was used for MCE and dSPM. The conductivity boundaries for the boundary element model were determined from MRI; only the inner surface of the skull is needed for MEG (Hämäläinen and Sarvas, 1989; Meijs and Peters, 1987; Meijs et al., 1987). The effect of the volume conductor model is expected to be minor in the present study. In general, the spherical model is quite accurate for MEG data: the error in the dipole location because of the spherical approximation as compared with more realistic head models is expected to be small, typically less than 1 cm (Hämäläinen and Sarvas, 1989; Leahy et al., 1998).

Equivalent current dipoles were calculated using the single-dipole model. All sensors were included in the analysis. The ECD that had the best goodness of fit (GOF) was selected as the representative ECD of that particular MEG spike. However, GOF is a measure of how well the ECD model explains the measured signals. A dipole fit was accepted when the GOF was more than 70%. The relatively low GOF threshold was chosen because only a few planar gradiometer MEG sensors show a prominent signal for a single source (Hämäläinen et al., 1993), and the inclusion of the sensors with little or no signal makes the GOF values lower than is typically seen when source localization is based on fewer channels or with axial gradiometers. The ECDs were superimposed on each patient's MRI to visualize their anatomical location.

For MCE, source distributions within the brain volume were estimated by assuming that they minimized the L1 norm, that is, the sum of the absolute values of the source amplitudes (Uutela et al., 1999). A characteristic feature of the maps obtained with the MCE method is that the patterns of estimated activity are relatively focal compared with the minimum L2-norm estimates. The MCE results were projected to the surface of the brain boundary for visualization.

The dSPM method is based on the generalized least squares or weighted minimum-norm estimate (Dale and Sereno, 1993; Hämäläinen and Ilmoniemi, 1994), which is normalized for noise sensitivity (Dale et al., 2000). The noise normalization provides a statistical parametric map, similar to the statistical maps typically generated using functional MRI or positron emission tomography data but with a millisecond temporal resolution. For the dSPM analysis, we used an anatomically constrained distributed source model, which assumed that the sources are located in the cerebral cortex. The cortical surface was segmented from the high-resolution MRI using FreeSurfer software (Dale et al., 1999; Fischl et al., 1999). The source model consisted of current dipole vectors at approximately 2,500 locations on the cortical surface in each hemisphere. The noise normalization reduces the variation in the point-spread function between locations (Liu et al., 2002). Simulations have suggested that the spatial resolution is 15 mm or better (Dale et al., 2000; Liu et al., 2002). The significance of modulation at each site was calculated using an *F*-test (Dale et al., 2000; Dhond et al., 2001). These statistical maps differ from maps of estimated source strengths because the estimated noise variance is not constant across different cortical locations. However, because the same noise covariance estimates are used at all time points for a given cortical location, the source strength at a given location over time are directly proportional to the statistical maps.

All source estimation was based on MEG data only; EEG data was inspected visually. The MEG data were digitally filtered with a pass band of 3 to 30 Hz for offline analysis. Segments containing abnormal paroxysms were selected manually. In addition to individual spikes, for some patients with localized spikes, we also analyzed averages of 10 to 20 spikes selected for their consistent sensor topography and aligned on the basis of their peak time. Equivalent current dipoles and dSPM maps were calculated at 2.5-millisecond intervals within a period of 100 milliseconds at the vicinity of each MEG spike. The MCE solutions were calculated for 20-millisecond time windows at and around the peak of each spike. Initially, we tried single time instants at 2.5-millisecond intervals for the MCE analysis as well; however, to improve the stability of the MCE solutions, averaging over a 20-millisecond time window was necessary. A potential caveat in smoothing the data by low-pass filtering and time window averaging is that one may diminish the early part of the IED that has been found to be important in determining the initial part of the activity (Ossenblok et al., 2007). In the present study, we mainly examined the activity during the peak of a spike.

Concordance of the MEG results provided by the three source localization methods (ECD, MCE, and dSPM) with a clinical hypothesis, based on semiology, EEG, and MRI, was determined at the hemispheric and lobar levels.

RESULTS

Patients With Localized Spikes

Concordant localization results were found between the ECD, MCE, and dSPM methods in patients 1, 2, and 3 with SLRE, in patient 4 with idiopathic localization–related epilepsy, and patient 5 with undetermined epilepsy (Table 1).

Patient 5 was an 8-year-old girl who had Landau–Kleffner syndrome with acquired aphasia accompanied by hemiconvulsive seizures (Fig. 1). This patient had frequent or continuous spikes [F1] dominantly at the left middle temporal and central regions in EEG and MEG. Equivalent current dipoles were located mainly in the left superior temporal gyrus, although some were located in the left inferior frontal gyrus (Fig. 1A). The direction of the ECDs suggests a temporal rather than a frontal origin. Minimum current estimate and dSPM suggested that most active area during the peak of the spike was in the superior temporal gyrus, with some simultaneous additional activity in the dSPM in the inferior frontal gyrus, adjacent to the superior temporal gyrus activity (Figs. 1B and 1C).

Patients With Diffuse Spikes

In patients 6, 7, 8, 9, and 10 with SLRE and in patient 11 with idiopathic localization–related epilepsy, qualitative differences were found between the ECD model and the distributed source estimates (MCE and dSPM). The distributed estimates suggested multifocal or widespread activations, sometimes with notable propagation over time, whereas the ECDs were either localized to one region only, widely scattered, or could not be calculated at all (Table 1).

Distributed source estimates for diffuse spikes are illustrated in Fig. 2. Patient 10 was an 8-year-old boy with tuberous sclerosis. MRI [F2] indicated multiple tubers in the frontal and parietal lobes. His seizures manifested as bilateral numbness of the foot, face, and eyeballs, evolving to complex gestural manual automatisms with impairment of consciousness. Diffuse spikes with slow waves over bilateral, but predominantly posterior, cerebral cortices could be seen in EEG. The ECDs were widespread over the right occipital and parietal lobes, and an exact epileptogenic focus could not be determined. Dynamic statistical parametric mapping suggested widespread activation of the right inferior and superior frontal gyri (Figs. 2A and 2C). Activity in these multiple areas appeared almost simultaneously and sometimes expanded within milliseconds over wide areas of the right frontal lobe

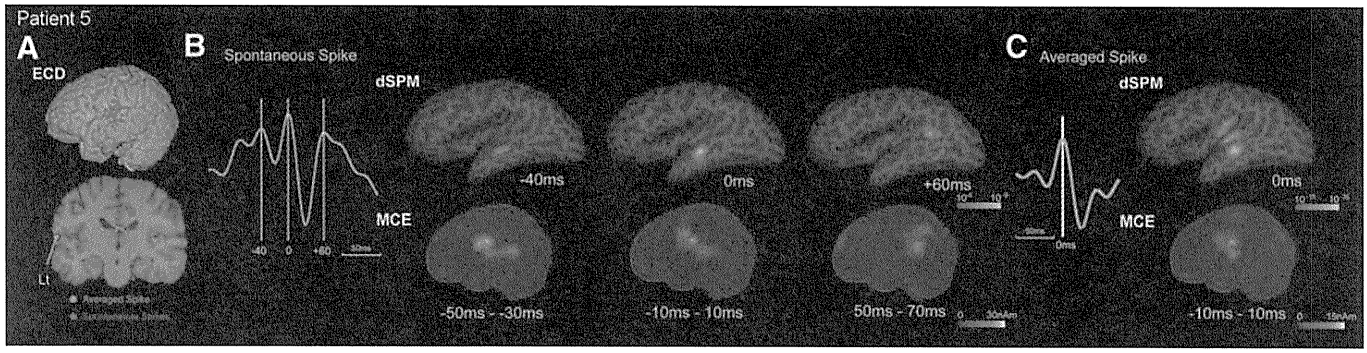

FIG. 1. Patient 5. Equivalent current dipole, dSPM, and MCE results for localized spikes in a patient with Landau–Kleffner syndrome. A, ECDs for individual spikes (red dots) were located in the left superior temporal gyrus and inferior frontal gyrus; ECD for the averaged spike was located in the left superior temporal gyrus (green dot). Only the peak point (0 milliseconds) was used for the analysis of the averaged spike. B, Dynamic statistical parametric mapping (top) and MCE (bottom) results for an individual spike. Dynamic statistical parametric mapping suggested activity in the left superior temporal gyrus at -40 milliseconds (left), in the same area more strongly at 0 milliseconds (middle) and near the left supramarginal gyrus at +60 milliseconds (right). Minimum current estimate showed activity in the left inferior frontal and superior temporal gyri at -50 to -30 milliseconds (left), in the same area at -10 to +10 milliseconds (middle), and near the left supramarginal gyrus at +50 to +70 milliseconds (right). C, Dynamic statistical parametric mapping (top) for the averaged spike suggested largest activation area at 0 milliseconds mainly in the left superior temporal gyrus and, additionally, in the lower operculum in the left frontal and parietal lobes, similar to the results for the individual spikes. Minimum current estimate(bottom) for the averaged spike also suggested largest activation in the left inferior frontal and superior temporal gyri at -10 to +10 milliseconds.

in the dSPM movies. In MCE, the most active area at the peak of the spike was in the supramarginal gyrus in the right parietal lobe, although an additional active area was seen in the left inferior frontal gyrus (Figs. 2B and 2D). These areas remained active after the peak, but the most active area moved to the left frontal lobe. However, the propagation in the right frontal areas seen in dSPM was not evident in MCE. The patient's seizure manifestation was thought to arise most likely from involvement of the frontal lobe, especially in the cingulate gyrus in the medial frontal lobe. Thus, the dSPM results were most concordant with his seizure manifestation.

Patients With Generalized Epilepsy

In patients 12, 13, and 14 with generalized epilepsy (GE), interictal EEG showed diffuse discharges and widespread activation was expected. In these three patients, reliable ECD results could not be obtained because the spikes were too widespread. The locations of the ECDs were scattered, and the GOF was low. Minimum current estimate and dSPM analyses suggested widespread activity, both simultaneous and propagating (Table 1).

[F3] Fig. 3 shows examples of distributed source estimates in a patient with GE. Patient 13 was 14 years old with Lennox–Gastaut syndrome who had tonic seizures and atypical absence seizures. His EEG showed two types of IED patterns: bilateral diffuse spike rhythm, and diffuse slow spike and wave complex. Gliosis was found in bilateral perisylvian and occipital regions supplied by the middle and posterior cerebral arteries in diagnostic MRI. This lesion was probably related to asphyxia during the perinatal period. The dSPM for both types of epileptiform discharges suggested that the largest activation during the spiking period was in both inferior frontal and superior temporal gyri bilaterally, which then suddenly propagated widely to the frontal and temporal lobes. The distribution of activity for the diffuse spike rhythm was wider than that for the diffuse spike and wave complex (Figs. 3A and 3C). Minimum current estimate of the above two epileptiform discharges showed separate regions of activity in the frontal and temporal lobes (Figs. 3B and 3D).

DISCUSSION

The three different source estimation methods (ECD, MCE, and dSPM) provided consistent results for very focal IEDs. In many cases with a less focal irritative zone, the distributed source estimates (MCE and dSPM) suggested multifocal or widespread activation that was in concordant with the patient's clinical symptoms. Typically, the single-ECD model was inadequate in these cases. Propagation of activity among multiple areas was often easier to detect and interpret using dSPM than using MCE, making dSPM a superior choice in these cases. The applicability and relative advantages of the different source estimation methods as a diagnostic tool assisting in syndrome classification in epilepsy are discussed below.

Localization of Focal Activity

Equivalent current dipoles have been the main method of analysis in MEG investigations of patients with epilepsy so far (Nakasato et al., 1994; Sutherling et al., 1987; Shiraishi et al., 2001; Stefan et al., 2000). Previously, the ECD localization of IEDs has been found to be closely correlated to the location of epileptogenic area in intracranial recordings (Oishi et al., 2006). The ECD method is a useful tool for localizing very focal activity that is restricted to a small region of the cortex. This is often the case, for example, with early sensory evoked responses, such as somatosensory evoked fields (Hari et al., 1993; Kakigi, 1994; Kawamura et al., 1996) or auditory evoked fields (Elberling et al., 1980; Hari et al., 1980; Pantev et al., 1990; Yamamoto et al., 1988). For example, an ECD model of somatosensory evoked fields can provide precise information about the position of the central sulcus, thereby helping to preserve the primary motor and sensory areas in surgery (Gallen AQ : 2 et al., 1995; Ishitobi et al., 2005; Inoue et al., 1999; Nakasato and Yoshimoto, 2000). The ECDs of the epileptic discharge can also give useful information about the relationship between the epileptogenic area and organic lesions (e.g., dysembryoplastic neuroepithelial tumor or focal cortical dysplasia), critical for defining the operative approach (Otsubo et al., 2001).

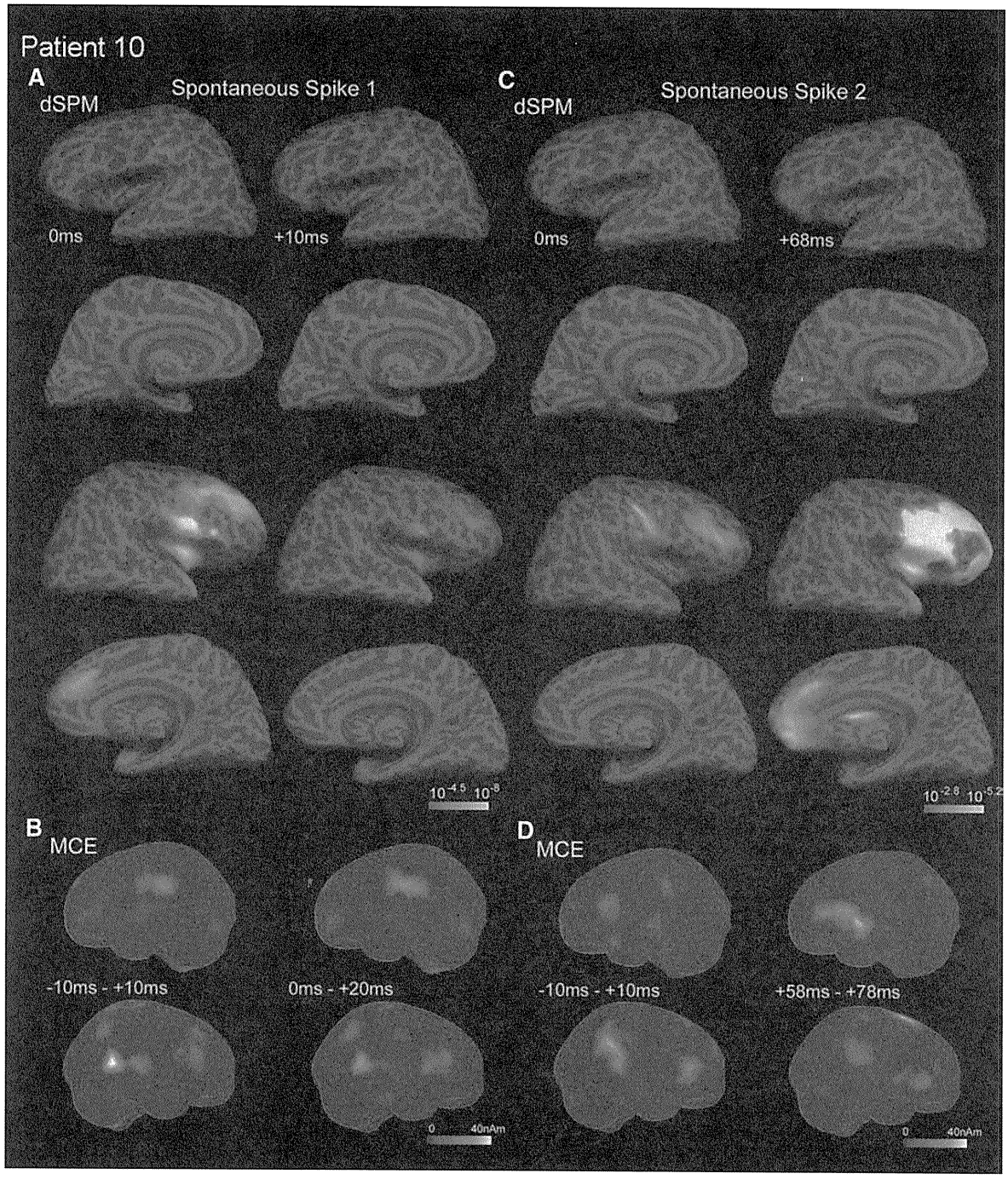

FIG. 2. Case 10. Dynamic statistical parametric mapping and MCE results for diffuse spikes. A, Dynamic statistical parametric mapping results for one spike (lateral and medial views of the left and right hemisphere). At the peak of the spike (0 milliseconds), dSPM suggested widespread simultaneous activation in the right inferior and superior frontal gyri. Weaker activity was also seen at the right anterior cingulate gyrus. The activation patterns remained similar after 10 milliseconds and did not propagate to another lobe. B, Minimum current estimate results for the same spike (lateral views of the left and right hemisphere). The MCE suggested largest activation in the right temporo–parieto–occipital junction (near the supramarginal and angular gyri), and minor activation in the right inferior Rolandic and left inferior frontal gyrus from -10 to +10 milliseconds. Activity in the right temporo–parieto–occipital junction was reduced, and left Rolandic activity was slightly increased, during the later period (0 to +20 milliseconds). C, For another spike, dSPM showed activation in the right Rolandic and inferior frontal gyri simultaneously at 0 milliseconds. The activity propagated over most of the right frontal lobe by +68 milliseconds. D, For the second spike, MCE showed largest activation around the right temporo–parieto–occipital junction and inferior frontal gyrus from –10 to +10 milliseconds. The active area in MCE moved to the right superior frontal and left inferior frontal gyri with multiple foci from +58 to +78 milliseconds.

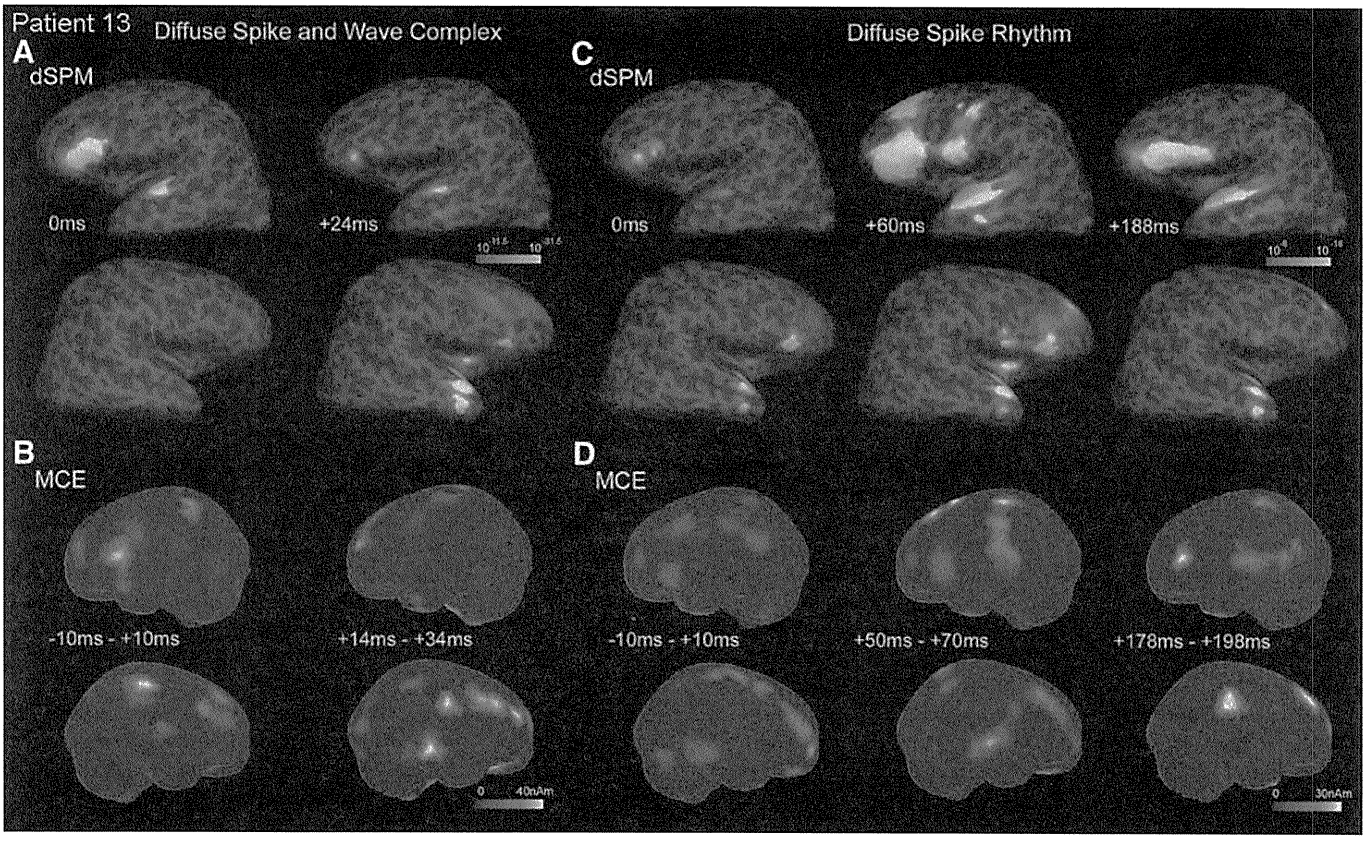

FIG. 3. Case 13. Dynamic statistical parametric mapping and MCE results for a diffuse spike and slow wave complex and diffuse spike rhythm. A, Dynamic statistical parametric mapping results for a diffuse spike and slow wave complex (lateral views of the left and right hemispheres). At the peak of the spike (0 milliseconds), the most active area was seen in the left inferior frontal and superior temporal gyri simultaneously. Later (24 milliseconds after the peak), dSPM spread to include right anterior temporal and prefrontal cortices. B, Minimum current estimate results for the same complex (lateral views of the left and right hemisphere). Minimum current estimate suggested several foci of activity over both the frontal and the parietal lobes, bilaterally, during the spike period (–10 to 10 milliseconds). For the later period (+14 to 34 milliseconds), multiple MCE foci are noted over the right frontal, central, and temporal areas and left frontal pole. C, Dynamic statistical parametric mapping results for a diffuse spike rhythm. Bilateral inferior frontal and anterior temporal activation of varying extent is seen at three successive spike peaks (0 +60 milliseconds and +188 milliseconds). D, Minimum current estimate results for the diffuse spike rhythm showed less consistent activation, predominantly over the right frontal lobe for the first spike (-10 to +10 milliseconds), over both frontal lobes, right temporal, and left central areas for the second spike (+50 to +70 milliseconds), and over bilateral frontal, left central, and right parietal areas for the third (+178 to +198 milliseconds).

For those patients in our study whose ECDs for IEDs were well clustered at one part in their brain (patients 1, 2, 3, 4, 5, 7, and 11), also, the distributed source estimates showed a localized maximum, indicating that the dSPM and the MCE can localize an abnormal epileptic focus. Typically, the peak location of a focus can be determined with higher precision than what is the spatial resolution of dissociating two separate foci, which has been found in simulations to be approximately 15 mm or better (Dale et al., 2000). An example of how MEG can provide valuable information can be seen by comparing patients 1 and 11. The distributed source estimates distinguished the difference in the abnormal areas between patient 1 with symptomatic frontal lobe epilepsy and patient 11 with atypical benign partial epilepsy in infancy, although their EEG findings seemed identical. The MEG-derived locations were concordant with the seizure type and epileptic syndrome of each patient.

Characterization of Multifocal and Widespread Activity

The single-ECD method may fail to give meaningful results in the case of widespread or propagating epileptic activity (see e.g., Hattori et al., 2001; Hisada et al., 2001; Shiraishi et al., 2005*a*; Oishi et al., 2006; Ossenblok et al., 1999). Clusters of ECDs may reflect both the initial and propagated activity (Bast et al., 2006; Ossenblok et al., 2007). An advantage of the dSPM and MCE methods is that in addition to the identification of multiple simultaneously active areas, the spatiotemporal maps can indicate dynamic changes in brain activity, thereby revealing patterns of propagation of the IEDs with high temporal resolution (Shiraishi et al., 2005*b*).

Previously, the dSPM technique has been used to analyze highly integrated brain activities related to cognitive tasks (Dale et al., 2000; Dhond et al., 2001); in these studies, dSPM identified activity occurring in various lobes simultaneously and multifocally.

Similarly, the MCE method has been successfully used for the analysis of a variety of event-related activity (Levanen et al., 2001; Raij et al., 2000; Rinne et al., 2000). The distributed source models allow detection of multiple simultaneously active areas, even when the single-ECD model may reveal only one active region or does not provide interpretable results at all (Shiraishi et al., 2005*b*). For example, in patient 10, dSPM suggested maximum activation at two separate locations: the lower part of the right motor strip and the premotor area. Such information could not be obtained with the single-ECD technique only. Furthermore, EEG findings also indicated widespread spikes, and the ECDs for the MEG data did not cluster well; however, the dSPM showed a consistent rather widespread epileptogenic region.

Propagation of activity was more difficult to identify in the MCE than in the dSPM solutions because the MCE solutions appeared to be sensitive to background noise, and the most active location in the MCE often suddenly changed between subsequent time points. Therefore, even if the most active areas were the same in the MCE and the dSPM at the peak of the epileptic spikes, the instability of the solution made it difficult to identify the propagation of the spikes in the MCE. The MCE results were similar to the dSPM ones mainly for the averaged spikes only. For example, the dSPM and the MCE differed in patients 10 and 13. In patient 10, the MCE showed the left frontal activity and did not show the spatiotemporal evolution of the interictal discharge, presumably because the MCE solution was influenced by the background noise. In patient 13, the dSPM did not show activation at the parietal region, hence the scattered MCE results in this case were interpreted as not reflective of significant activation.

Minor differences between the dSPM and MCE results were because of the different definition of the source space (i.e., the cortical surface in dSPM versus the brain volume in MCE). For example, MCE did not indicate activity in the medial frontal lobe in patient 2 and in the medial structure or perisylvian area in patient 3 because the version of the MCE software used in the present study did not include the medial surfaces in the visualization of the results. These were specific properties of the software that was available to us; however, there is no reason in principle why the same source space could not be used for dSPM and MCE. It would be interesting to compare the present results with those obtained with modified MCE methods with temporally and spatially smooth solutions (Huang et al., 2006).

The dSPM maps were often found to show more widespread source estimates for averaged spikes than for individual spikes. A likely explanation for this was the overall increase in signal-to-noise ratio for averaged spikes, which is what is depicted by the dSPM maps: a lower level of noise provided a more reliable detection of the spike itself but does not significantly affect the spatial pattern of the background noise in the data, only the noise amplitude is reduced. Therefore, in the noise-normalized maps, a wider portion around the peak activation, caused by the point-spread function of the inverse solution (Dale et al., 2000), is above the visualization threshold.

The interpretation of our results was limited by the lack of independent validation of the true pattern of activation. Our MEG studies were performed for diagnostic purposes only, not for presurgical evaluation. Therefore, the results have not been validated by invasive monitoring or postsurgical outcome. However, comparison of the ECD, MCE, and dSPM results with the seizure semiology and MRI findings suggested the feasibility of the advanced distributed source estimation approaches in characterizing widespread and propagating activity for the purpose of syndrome classification in epilepsy.

Because the ECD technique has been the main method for the analysis of MEG data, typically, only patients with SLRE whose epileptiform activity was anticipated to be focal in onset have been studied with MEG. The dSPM technique could also be useful for the analysis of diffuse spikes or slow waves, even when both hemispheres are involved (Shiraishi et al., 2005*a*). The dSPM technique also suggested bilateral diffuse discharges in both hemispheres in the patients with GE, such as patients 13 and 14. Our results from patient 13 with Lennox–Gastaut syndrome, however, are not concordant with the results of MEG and EEG–functional MRI studies in patients with idiopathic generalized epilepsy (absence epilepsy), which show involvement of bilateral frontal and posterior temporal or parietal regions and middle frontal regions (Moeller et al., 2010; Westmijse et al., 2009). It is possible that the localization results for this patient correspond not to absence seizure but to more diffuse epileptic paroxysms. Although we have no validation of the difference, dSPM might indicate a clinical difference among patients with GE. The diagnosis of the epileptic syndrome is usually based on EEG findings and clinical manifestations. Our present study suggests that the dSPM technique could make the MEG examination more widely applicable, not only for SLRE but also for GE. The temporal and spatial resolution of dSPM may suggest the mechanism of epileptogenesis (e.g., dSPM helped differentiate the epileptic syndromes of patient 11 as focal and 13 as generalized), although the EEGs of both patients were diffuse spikes.

The ability of the dSPM method to characterize widespread and propagating activity suggests that the dSPM may be suitable also for the analysis of IDs as well as IEDs. For the diagnosis of the epileptic syndrome, IDs can provide valuable information. Earlier, the application of MEG for IDs in patients with epilepsy was limited by small sensor arrays that covered only a part of the brain (Oishi et al., 2002; Shiraishi et al., 2001; Shigeto et al., 1997; Uesaka et al., 1996; Watanabe et al., 1996). The availability of helmet-shaped multi–superconducting quantum interference device systems makes it possible to detect the IDs over most of the brain. For these types of data, distributed source estimates, such as the dSPM, are clearly expected to be superior.

Our current results provide evidence of the usefulness of analyzing MEG data with methods that go beyond the ECD, warranting further evaluation of these methods in future studies. We hypothesize that for clinical applications, an initial spatial filtering analysis, such as dSPM, could indicate whether the epileptic discharge is focal or diffuse. If the activity is focal, ECD analysis is expected to provide valuable localization information. If the activity is diffuse, examination of the dSPM movie will suggest how the discharge propagates over space and time.

ACKNOWLEDGMENTS

The authors thank Gregory Kirk, Maureen Glessner, Mark Halko, and Thomas Witzel for technical support.

REFERENCES

Aicardi J, Chevrie JJ. Atypical benign epilepsy of childhood. *Dev Med Child Neurol* 1982;24:281–292.

Adelson PD, Black PM, Madsen JR, et al. Use of subdural grids and strip electrodes to identify a seizure focus in children. *Pediatr Neurosurg* 1995;22:174–180.

Baillet S, Mosher JC, Leahy M. Electromagnetic brain mapping. *IEEE Signal Proc Mag* 2001;18:14–30.

Bast T, Boppel T, Rupp A, et al. Noninvasive source localization of interictal EEG spikes: effects of signal-to-noise ratio and averaging. *J Clin Neurophysiol* 2006;23:487–497.

Baumgartner C, Lindinger G, Ebner A, et al. Propagation of interictal epileptic activity in temporal lobe epilepsy. *Neurology* 1995;45:118–122.
Blume WT. Current trends in electroencephalography. *Curr Opin Neurol* 2001;14:193–197.
Cascino GD, Trenerry MR, So EL, et al. Routine EEG and temporal lobe epilepsy: relation to long-term EEG monitoring, quantitative MRI, and operative outcome. *Epilepsia* 1996;37:651–656.
Cendes F, Li LM, Watson C, et al. Is ictal recording mandatory in temporal lobe epilepsy? Not when the interictal electroencephalogram and hippocampal atrophy coincide. *Arch Neurol* 2000;57:497–500.
Commission on Classification and Terminology of the International League Against Epilepsy. Proposal for revised classification of epilepsies and epileptic syndromes. *Epilepsia* 1989;30:389–399.
Dale AM, Sereno MI. Improved localization of cortical activity by combining EEG and MEG with MRI cortical surface reconstruction: a linear approach. *J Cogn Neurosci* 1993;5:162–176.
Dale AM, Fischl B, Sereno MI. Cortical surface-based analysis. I. Segmentation and surface reconstruction. *Neuroimage* 1999;9:179–194.
Dale AM, Liu AK, Fischl BR, et al. Dynamic statistical parametric mapping: combining fMRI and MEG for high-resolution imaging of cortical activity. *Neuron* 2000;26:55–67.
Danielpour M, Peacock WJ. Epilepsy surgery in children. *Clin Neurosurg* 2000;47:400–421.
deMunck JC. A linear discretization of the volume conductor boundary integral equation using analytically integrated elements. *IEEE Trans Biomed Eng* 1992;39:986–990.
Dhond RP, Buckner RL, Dale AM, et al. Spatiotemporal maps of brain activity underlying word generation and their modification during repetition priming. *J Neurosci* 2001;21:3564–3571.
Doherty CP, Cole AJ. The requirement for ictal EEG recordings prior to temporal lobe epilepsy surgery. *Arch Neurol* 2001;58:678–680.
Duchowny M, Jayakar P, Koh S. Selection criteria and preoperative investigation of patients with focal epilepsy who lack a localized structural lesion. *Epileptic Disord* 2000;2:219–226.
Ebersole JS, Pacia SV. Localization of temporal lobe foci by ictal EEG patterns. *Epilepsia* 1996;37:386–399.
Elberling C, Bak C, Kofoed B, et al. Magnetic auditory responses from the human brain. A preliminary report. *Scand Audiol* 1980;9:185–190.
Fischl B, Sereno MI, Tootell RB, et al. High-resolution intersubject averaging and a coordinate system for the cortical surface. *Hum Brain Mapp* 1999;8:272–284.
Gallen CC, Schwartz BJ, Bucholz RD, et al. Presurgical localization of functional cortex using magnetic source imaging. *J Neurosurg* 1995;82:988–994.
Gastaut H, Roger J, Soulayrol R, et al. Childhood epileptic encepharography with diffuse slow spike-waves (otherwise known as 'petit mal variant') or Lennox syndrome. *Epilepsia* 1966;7:139–179.
Gevins A, Le J, Martin NK, et al. High resolution EEG: 124-channel recording, spatial deblurring and MRI integration methods. *Electroencephalogr Clin Neurophysiol* 1994;90:337–358.
Hämäläinen MS, Ilmoniemi RJ. Interpreting magnetic fields of the brain: minimum norm estimates. *Med Biol Eng Comput* 1994;32:35–42.
Hämäläinen MS, Sarvas J. Realistic conductivity geometry model of the human head for interpretation of neuromagnetic data. *IEEE Trans Biomed Eng* 1989;36:165–171.
Hämäläinen M, Hari R, Ilmoniemi RJ, et al. Magnetoencephalography: theory, instrumentation, and application to noninvasive studies of the working human brain. *Rev Mod Phys* 1993;65:413–497.
Hari R, Aittoniemi K, Jarvinen ML, et al. Auditory evoked transient and sustained magnetic fields of the human brain. Localization of neural generators. *Exp Brain Res* 1980;40:237–240.
Hari R, Karhu J, Hamalainen M, et al. Functional organization of the human first and second somatosensory cortices: a neuromagnetic study. *Eur J Neurosci* 1993;5:724–734.
Hattori H, Yamano T, Tsutada T, et al. Magnetoencephalography in the detection of focal lesions in West syndrome. *Brain Dev* 2001;23:528–532.
Hisada K, Morioka T, Nishio S, et al. Two magneto-encephalographic epileptic foci did not coincide with the electrocorticographic ictal onset zone in a patient with temporal lobe epilepsy. *Neurol Res* 2001;23:830–834.
Hjorth B. EEG analysis based on time domain properties. *Electroencephalogr Clin Neurophysiol* 1970;29:306–310.
Huang MX, Dale AM, Song T, et al. Vector-based spatial-temporal minimum L1-norm solution for MEG. *Neuroimage* 2006;31:1025–1037.
Humphrey DR. Re-analysis of the antidromic cortical response. II. On the contribution of cell discharge and PSPs to the evoked potentials. *Electroencephalogr Clin Neurophysiol* 1968;25:421–442.
Inoue T, Shimizu H, Nakasato N, et al. Accuracy and limitation of functional magnetic resonance imaging for identification of the central sulcus: comparison with magnetoencephalography in patients with brain tumors. *Neuroimage* 1999;10:738–748.
Ishitobi M, Nakasato N, Yoshimoto T, et al. Abnormal primary somatosensory function in unilateral polymicrogyria: an MEG study. *Brain Dev* 2005;27: 22–29.
Kakigi R. Somatosensory evoked magnetic fields following median nerve stimulation. *Neurosci Res* 1994;454–457.
Kawamura T, Nakasato N, Seki K, et al. Neuromagnetic evidence of pre- and postcentral cortical sources of somatosensory evoked responses. *Electroencephalogr Clin Neurophysiol* 1996;100:44–50.
Knake S, Halgren E, Shiraishi H, et al. The value of multichannel MEG and EEG in the presurgical evaluation of 70 epilepsy patients. *Epilepsy Res* 2006; 69:80–86.
Ko DY, Kufta C, Scaffidi D, et al. Source localization determined by magnetoencephalography and electroencephalography in temporal lobe epilepsy: comparison with electrocorticography: technical case report. *Neurosurgery* 1998;42:414–422.
Landau WM, Kleffner FR. Syndrome of acquired aphasia with convulsive disorder in children. *Neurology* 1957;7:523–530.
Leahy RM, Mosher JC, Spencer ME, et al. A study of dipole localization accuracy for MEG and EEG using a human skull phantom. *Electroencephalogr Clin Neurophysiol* 1998;107:159–173.
Levanen S, Uutela K, Salenius S, et al. Cortical representation of sign language: comparison of deaf signers and hearing non-signers. *Cereb Cortex* 2001;11:506–512.
Liu AK, Belliveau JW, Dale AM. Spatiotemporal imaging of human brain activity using fMRI constrained MEG data: Monte Carlo simulations. *Proc Natl Acad Sci U S A* 1998;95:8945–8950.
Liu AK, Dale AM, Belliveau JW. Monte Carlo simulation studies of EEG and MEG localization accuracy. *Hum Brain Mapp* 2002;16:47–62.
Madsen JR, Adelson PD, Haglund MM. The future of pediatric epilepsy surgery. Signposts and science. *Neurosurg Clin N Am* 1995;6:589–597.
Matsuura K, Okabe Y. A robust reconstruction of sparse biomagnetic sources. *IEEE Trans Biomed Eng* 1997;44:720–726.
Meijs JWH, Peters MJ. The EEG and MEG: using a model of eccentric spheres to describe the head. *IEEE Trans Biomed Eng* 1987;34:913–920.
Meijs JWH, Bosch FGC, Peters MJ, et al. On the magnetic field distribution generated by a dipolar current source situated in a realistically shaped compartment model of the head. *Electroencephalogr Clin Neurophysiol* 1987;66: 286–298.
Moeller F, Siebner HR, Wolff S, et al. Changes in activity of striato-thalamo-cortical network precede generalized spike wave discharges. *Neuroimage* 2008;39: 1839–1849.
Nakasato N, Levesque MF, Barth DS, et al. Comparisons of MEG, EEG, and ECoG source localization in neocortical partial epilepsy in humans. *Electroencephalogr Clin Neurophysiol* 1994;91:171–178.
Nakasato N, Yoshimoto T. Somatosensory, auditory, and visual evoked magnetic fields in patients with brain diseases. *J Clin Neurophysiol* 2000;17:201–211.
Nordli DR Jr. Epilepsy surgery in children, with special attention to focal cortical resections. *Semin Pediatr Neurol* 2000;7:204–215.
Nunez PL, ed. *Electric fields of the brain*. New York: Oxford University, 1981.
Oishi A, Tobimatsu S, Ochi H, et al. Paradoxical lateralization of parasagittal spikes revealed by back averaging of EEG and MEG in a case with epilepsia partialis continua. *J Neurol Sci* 2002;193:151–155.
Oishi M, Kameyama S, Masuda H, et al. Single and multiple clusters of magnetoencephalographic dipoles in neocortical epilepsy: significance in characterizing the epileptogenic zone. *Epilepsia* 2006;47:355–364.
Oostendorp TF, van Oosterom A. Source parameter estimation in inhomogeneous volume conductors of arbitrary shape. *IEEE Trans Biomed Eng* 1989;36:382–391.
Ossenblok P, Fuchs M, Velis DN, et al. Source analysis of lesional frontal-lobe epilepsy. *IEEE Eng Med Biol Mag* 1999;18:67–77.
Ossenblok P, de Munck JC, Colon A, et al. Magnetoencephalography is more successful for screening and localizing frontal lobe epilepsy than electroencephalography. *Epilepsia* 2007;48:2139–2149.
Otsubo H, Ochi A, Elliott I, et al. MEG predicts epileptic zone in lesional extrahippocampal epilepsy: 12 pediatric surgery cases. *Epilepsia* 2001;42: 1523–1530.
Pantev C, Hoke M, Lehnertz K, et al. Identification of sources of brain neuronal activity with high spatiotemporal resolution through combination of neuromagnetic source localization (NMSL) and magnetic resonance imaging (MRI). *Electroencephalogr Clin Neurophysiol* 1990;75:173–184.
Pedley T. Epilepsy and the human electroencephalogram. In: Schwartzkroin P, Wheal H, eds. *Pathophysiology of epilepsy*. London: Academic Press, 1984: 1–30.
Penfield W, Jasper H, eds. *Epilepsy and the Functional Anatomy of the Human Brain*. Boston: Little, Brown and Company, 1954.
Raij T, Uutela K, Hari R. Audiovisual integration of letters in the human brain. *Neuron* 2000;28:617–625.
Rinne T, Alho K, Ilmoniemi RJ, et al. Separate time behaviors of the temporal and frontal mismatch negativity sources. *Neuroimage* 2000;12:14–19.
Rosenow F, Lüders H. Presurgical evaluation of epilepsy. *Brain* 2001;124: 1683–1700.

AQ : 4
AQ : 5

Scherg M. Functional imaging and localization of electromagnetic brain activity. *Brain Topogr* 1992;5:103–111.
Scherg M, Bast T, Berg P. Multiple source analysis of interictal spikes: goals, requirements, and clinical value. *J Clin Neurophysiol* 1999;16:214–224.
Shigeto H, Tobimatsu S, Morioka T, et al. Jerk-locked back averaging and dipole source localization of magnetoencephalographic transients in a patient with epilepsia partialis continua. *Electroencephalogr Clin Neurophysiol* 1997;103: 440–444.
Shiraishi H, Watanabe Y, Watanabe M, et al. Interictal and ictal magnetoencephalographic study in patients with medial frontal lobe epilepsy. *Epilepsia* 2001;42:875–882.
Shiraishi H, Ahlfors SP, Stufflebeam SM, et al. Application of magnetoencephalography in epilepsy patients with widespread spike or slow-wave activity. *Epilepsia* 2005a;46:1264–1272.
Shiraishi H, Stufflebeam SM, Knake S, et al. Dynamic statistical parametric mapping for analyzing the magnetoencephalographic epileptiform activity in patients with epilepsy. *J Child Neurol* 2005b;20:363–369.
Spencer SS. The relative contributions of MRI, SPECT, and PET imaging in epilepsy. *Epilepsia* 1994;35:S72–S89.
Spencer SS, Bautista RE. Functional neuroimaging in localization of the ictal onset zone. *Adv Neurol* 2000;83:285–296.
Stefan H, Hummel C, Hopfengartner R, et al. Magnetoencephalography in extratemporal epilepsy. *J Clin Neurophysiol* 2000;17:190–200.
Sutherling WW, Crandall PH, Engel J Jr, et al. The magnetic field of complex partial seizure agrees with intracranial localizations. *Ann Neurol* 1987;21: 548–558.
Uesaka Y, Terao Y, Ugawa Y, et al. Magnetoencephalographic analysis of cortical myoclonic jerks. *Electroencephalogr Clin Neurophysiol* 1996;99:140–148.
Uutela K, Hämäläinen M, Somersalo E. Visualization of magnetoencephalographic data using minimum current estimates. *Neuroimage* 1999;10:173–180.
Watanabe Y, Fukao K, Watanabe M, et al. Epileptic events observed by multichannel MEG. In: Hashimoto I, ed. *Visualization of information processing in the human brain*. Amsterdam: Elsevier, 1996:383–392.
Westmijse I, Ossenblok P, Gunning B, *et al*. Onset and propagation of spike and slow wave discharges in human absence epilepsy: a MEG study. *Epilepsia* 2009;50:2538–2548.
Yamamoto T, Williamson SJ, Kaufman L, et al. Magnetic localization of neuronal activity in the human brain. *Proc Natl Acad Sci U S A* 1988;85:8732–8736.

ELSEVIER

Brain & Development 33 (2011) 276–281

BRAIN & DEVELOPMENT
Official Journal of the Japanese Society of Child Neurology

www.elsevier.com/locate/braindev

Original article

Source localization in magnetoencephalography to identify epileptogenic foci

Hideaki Shiraishi *

Department of Pediatrics, Hokkaido University, Graduate School of Medicine, Japan

Received 1 August 2010; received in revised form 21 October 2010; accepted 22 October 2010

Abstract

Rationale: Magnetoencephalography (MEG) is useful to localize epileptic foci in epilepsy as MEG has higher spatio-temporal resolution than conventional diagnostic imaging studies; positron emission computed tomography, single photon emission computed tomography and magnetic resonance imaging (MRI).

Methods: We use 204-channel helmet-shaped MEG with a sampling rate of 600 Hz. A single dipole method calculates equivalent current dipoles to localize epileptic sources. The equivalent current dipoles are superimposed onto MRI as magnetic source imaging (MSI). Ictal MEG data are analyzed using time–frequency analysis. The power spectrum density is calculated using short-time Fourier transform and superimposed onto MRI results.

Results: Clustered equivalent current dipoles represent epileptogenic zones in patients with localization-related epilepsy. The surgical plan is reliably developed from source localizations of dipoles and power spectrum of interictal spike discharges, and ictal frequency.

Conclusion: MEG is indispensable in diagnosis and surgical resection for epilepsy to accurately localize the epileptogenic zone.

Keywords: Magnetoencephalography; Epilepsy; Single dipole method; Time–frequency analysis; Short-time Fourier transform analysis

1. Introduction

Magnetoencephalography (MEG) arose originally from investigations into superconductivity and its subsequent practical application in the measurement of weak electric fields. The technique is now used clinically [1,2]. Magnetoencephalography is particularly useful in studying epileptic disorders, as it provides better spatial and temporal resolution than electroencephalography (EEG) for the localization of pathological brain activity or lesions.

Many reports describe the application of MEG in the clinical investigation of epileptic patients [3–9]. Magnetoencephalography also currently has an important role in defining epileptogenic lesions in epilepsy surgery candidates, especially those with neocortical epileptic lesions [10–14]. In the present study, we report the efficiency of MEG in the diagnosis of two epileptic syndromes.

2. Methods

2.1. MEG data acquisition

MEG data were recorded using 204-channel helmet-shaped gradiometers (Vector View, Elekta, Stockholm, Sweden) at a 600 Hz sampling rate. The MEG data were digitally filtered with a band-pass from 3 to 30 Hz for offline analysis. Segments containing abnormal paroxysms were identified manually.

* Address: North15 West7, Kita-ku, Sapporo, Hokkaido 060-8638, Japan. Tel.: +81 11 706 5954; fax: +81 11 706 7898.
E-mail address: siraisi@med.hokudai.ac.jp

0387-7604/$ - see front matter © 2010 The Japanese Society of Child Neurology. Published by Elsevier B.V. All rights reserved.
doi:10.1016/j.braindev.2010.10.019

2.2. Equivalent current dipole

Individual spikes were aligned on the basis of the peak latency and analyzed. The distribution of brain activity generating the spikes was determined using a source estimation approach; the equivalent current dipole (ECD) model. This model is appropriate when the underlying brain activity is focal, i.e. restricted to a relatively small region of the brain.

Equivalent current dipoles were calculated with xfit software (Elekta Neuromag Ltd.,) using the single dipole model. The conductivity geometry of the head was assumed to be spherical and symmetrical. Dipoles were calculated for each time point measurement (every 2.5 ms) within 100 ms of each MEG spike. Results from all sensors were analyzed, with no regions of interest selected. The initial location for the iterative ECD fit was assumed to be under the sensor with the largest signal, and the ECD with the best goodness of fit (GOF) was selected as being representative of that particular MEG spike. The GOF is a measure of how well the ECD model explains the measured signals. A dipole fit was accepted when the GOF was greater than 70%. To visualize anatomical locations, the ECDs were superimposed on the MRI generated for each patient.

2.3. Short-time Fourier transform analysis

Short-time Fourier transform (STFT) analysis may be used to reveal the distribution of MEG polyspikes [15]. The MATLAB (MathWorks, Natick, USA) program was used to execute the STFT for the MEG signals. Each signal was divided into small sequential frames, and fast Fourier transformation (FFT) applied to each frame.

In the present study, the STFT was implemented using a 256-point window. The duration of each window was 426.7 ms (i.e. 256 points × 1000 ms/600 Hz). The window was shifted every four points, corresponding to 6.7 ms (i.e. 1000 ms/600 Hz × 4 points). The fast Fourier transform method was applied to each window. This process was repeated for all representative signals. The time–frequency distributions were displayed as graphs.

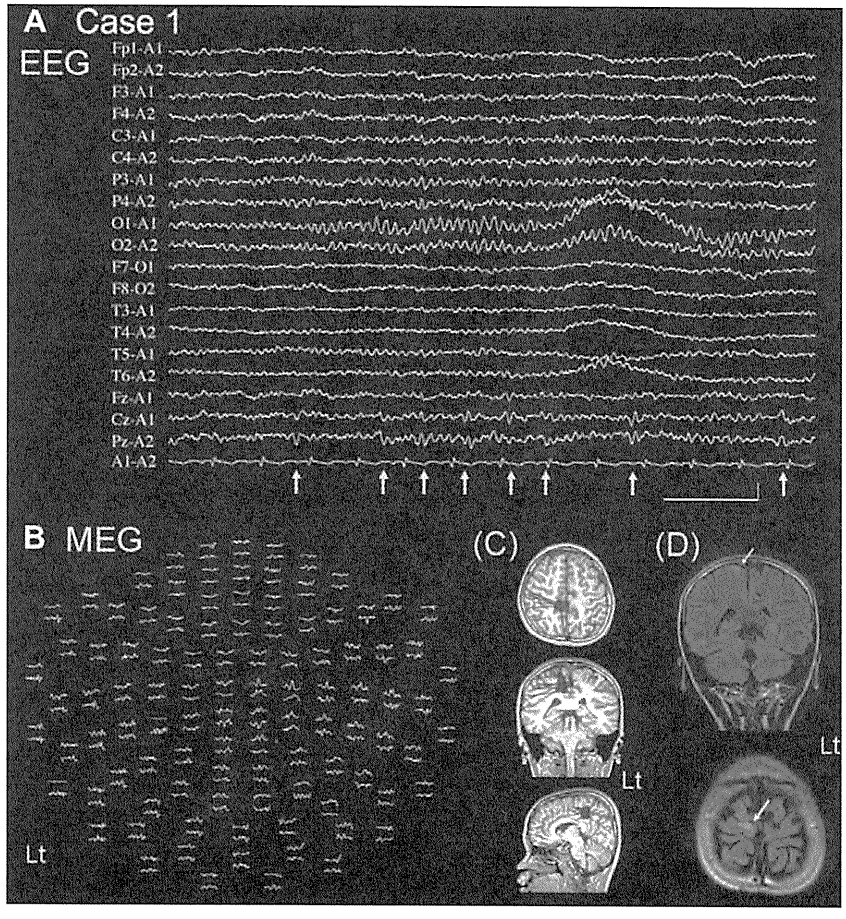

Fig. 1. EEG, MEG and MRI of case 1. (A) EEG showed interictal spikes on readings from Fz and Cz electrodes (white arrows). (B) MEG showed spikes in the right frontal area. (C) Equivalent current dipoles from MEG were localized to the top of the primary motor area in the right frontal lobe (red dots). (D) FLAIR MRI image showed high signal region at the top of the primary motor area in the right frontal lobe (yellow arrows).

Fast Fourier transform was performed for frequencies in the ranges of 3–30 Hz, 30–50 Hz, and 50–100 Hz. A signal's spectrum was considered to be aberrant when it was isolated from the background frequency spectrum in the graph. Such aberrant frequency spectra were superimposed onto the 3D magnetic resonance imaging (MRI) reconstruction.

3. Case reports

3.1. Case 1

A 13-year-old boy whose seizures first occurred at the age of 10 years, and began with focal motor seizures in the left leg and foot. His seizures evolved until, by the age of 13 years, they developed into a form of continuous focal seizure or epilepsia partialis continua. Sometimes these focal seizures progressed into secondary generalized tonic–clonic seizures. Electroencephalography (EEG) demonstrated intermittent spikes in recordings from the Cz and Fz electrodes, and MEG showed corresponding spikes at the top of the left frontal lobe (Fig. 1A). Equivalent current dipoles were located at the top of primary motor area in the left frontal lobe (Fig. 1B and C). A MEG-guided MRI scan showed a T2WI high intensity area at the top of left frontal lobe that corresponded to the clustered ECDs calculated following analysis of MEG data (Fig. 1D). Antiepileptic drugs were administrated to control the patient's seizures; however, cortical resection is planned as he still has daily seizures.

3.2. Case 2

An 11-year-old girl had, immediately following her birth, been presented with right hemiplegia. A computed tomography (CT) scan showed a stroke lesion due to congenital thrombosis of the left middle cerebral artery (Fig. 2A). Her seizures initially occurred at the age of 3 years. These seizures were postural, and resolved on decumbency. The seizures were described as involving extension of the patient's right arm and leg, contraction of the left arm and leg, and upward eye deviation.

Her interictal EEG showed spikes, as well as spikes with slow waves in the F3, Fp1, and F7 electrode data. MEG demonstrated epileptic spikes in the left frontal lobe, and ECDs localized near to the infarct in the left frontal lobe (Fig. 2B).

Ictal EEG showed slow waves in the left frontal recording, followed by left frontal dominant polyspikes. Ictal MEG data 4.0 s prior to ictal motion artifact was analyzed using STFT, and demonstrated left frontal

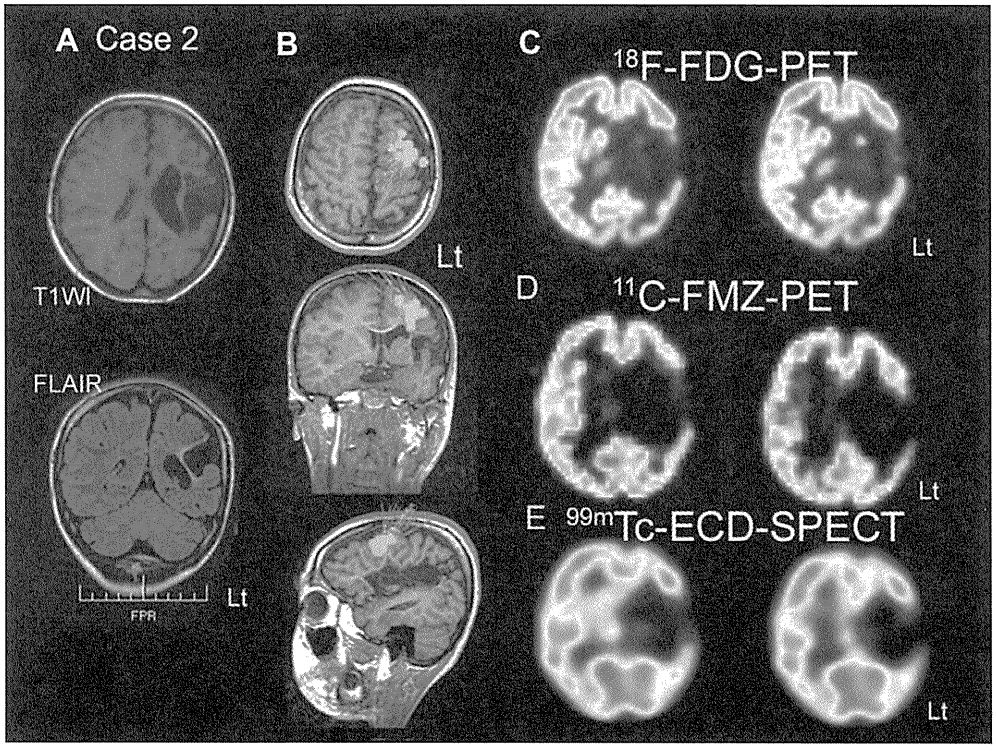

Fig. 2. MRI, MEG, PET and SPECT of case 2. (A) Axial and sagittal MR images demonstrated a congenital middle cerebral artery stroke in the left hemisphere. (B) Equivalent current dipoles from MEG study with clustered spike source localization near a stroke lesion in the left frontal lobe (green dots). (C) [18F]-fluorodeoxyglucose (FDG) positron emission CT (PET) showed hypofunctional glucose metabolism in the left frontal lobe. (D) [11C]-flumazenil (FMZ) PET showed reduction of the benzodiazepine receptor binding in the left frontal lobe. (E) 99m-Tc ethylcysteinate dimer (ECD) single photon emission CT (SPECT) showed hypoperfusion in the left frontal lobe.

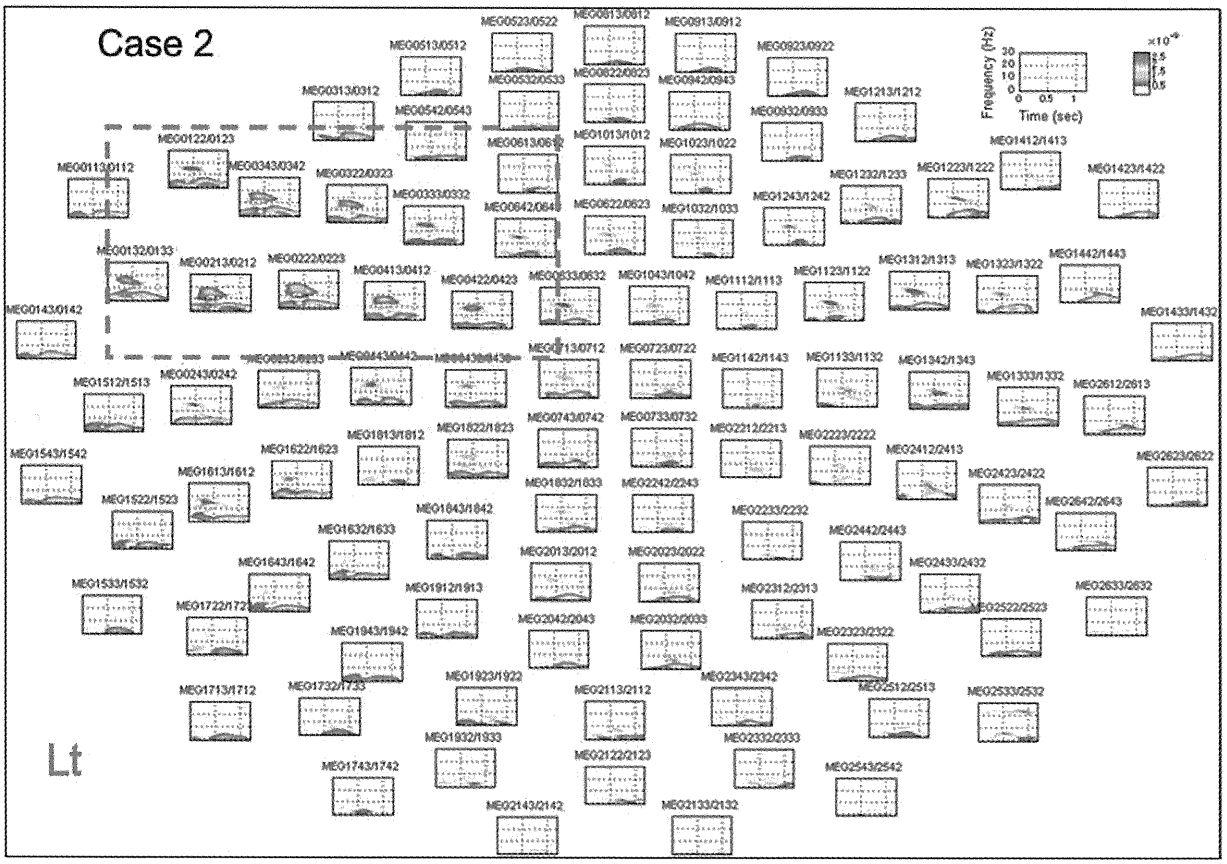

Fig. 3. STFT analysis in case 2. STFT showed aberrant magnetological oscillation in the left occipital and temporal and frontal areas at 7–12 Hz (surrounded by red lines).

dominant, rhythmic magnetological activity of 7–12 Hz (Fig. 3). These areas of high magnitude activity were located in the left superior frontal gyrus on 3D MRI (Fig. 4), which was consistent with the spike sources estimated using the single dipole method (SDM) (Fig. 5).

After noninvasive presurgical evaluation, the patient underwent long-term intracranial EEG monitoring using subdural electrodes. Electrical stimulation near the left premotor area induced her usual seizure. She underwent frontal lobectomy, including areas where high magnitude activity in ictal MEG data had been recorded (Fig. 5). She has been seizure free for the year following surgery, and has no mental or motor deficits.

4. Discussion

MEG has become an indispensable diagnostic tool for patient evaluation prior to neocortical epileptic

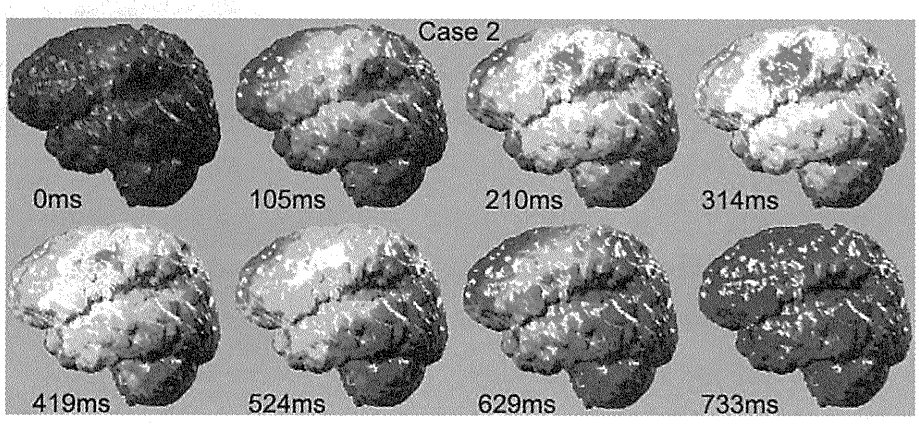

Fig. 4. MEG signal combined with the 3D MRI image in case 2. Aberrant oscillation generated from the top of the encephalomalacic areas at 105 ms with maximum power spectrum at 314 ms.

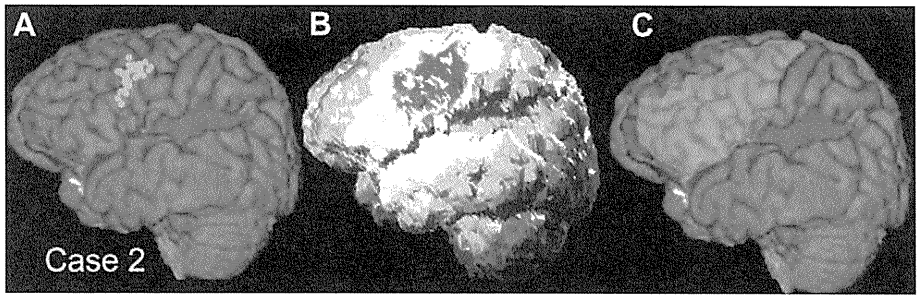

Fig. 5. MEG spike sources, maximum power spectrum of STFT and resected area in case 2. (A) MEG spike sources (green dots) were located in the middle frontal gyrus near to the encephalomalacic region (pink area). (B) The maximum power spectrum of the STFT analysis was located in the comparable area to that from which MEG spike sources (red area) were mapped. (C) Area of the cortical resection of the left frontal lobe (yellow area) which excluded the precentral gyrus.

surgery. This was demonstrated by the accurate localization of epileptogenic lesions in our two case studies. In patient 1, the MEG data also demonstrated a strong epileptogenic region and predicted a cortical lesion in the left frontal lobe. Hence, the high spatial resolution of MEG provided valuable information in the diagnosis of the epileptic syndrome in this case. The MEG data from patient 2 demonstrated a restricted and clustered epileptogenic focus resulting from a widespread cortical lesion, resulting from a congenital stroke in the cerebral cortex. MEG thus indicated the site of the cortical resection required for successful treatment of this patient.

This study has also shown the usefulness of MEG in identifying the ictogenic area in patients through investigations into epileptic rhythmic activity. Recently, Sueda et al. and Yagyu et al. described the clinical value of MEG oscillation analysis, and confirmed the efficacy of this method for pre and postoperative evaluation of epileptic patients [16,17].

The location of an ECD can be calculated only when a 3 cm^2 or wider area of cerebral cortex is synchronously activated [18]. Therefore, to obtain a suitable ECD, the activated areas of the cortex should be restricted in the analysis. This allows SDM to be applied to signals which have a good signal to noise ratio in comparison to background cortical activity. The SDM uses an inverse problem formula based on the hypothesis that the spike is generated from a localized area. Hence, SDM has limitations in its use in the evaluation of epileptic paroxysmal discharges, and is not applicable in cases with widespread cortical activity and propagated ictal activity with low amplitude recruiting of rhythmic activity. In contrast, time–frequency analysis has an advantage over the single dipole method, as there is no need to solve the inverse problem and define a region of interest for evaluation of these discharges.

Ictal rhythmic activity specifically shows the epileptogenic focus, especially using electrocorticography (ECoG). However in this study, MEG showed equivalent diagnostic usefulness for definition of the ictal onset zone, and unlike ECoG, is a noninvasive technique [19,20]. Thus, MEG potentially has an advantage over ECoG in pediatric patients, in whom long-term invasive monitoring is not possible. Further, MEG can simultaneously detect whole cortical activity, while investigation of the region of interest is limited in ECoG to the area of the craniotomy.

This study has confirmed MEG analysis is an invaluable tool in the diagnosis of epileptic syndromes and in presurgical evaluation. This study was presented at the 10th Asian & Oceanian Congress of Child Neurology in Daegu, Korea, which was held on June 10-13th, 2009.

References

[1] Cohen D. Magnetoencephalography: evidence of magnetic fields produced by alpha-rhythm currents. Science 1968;161:784–6.
[2] Hamäläinen M, Hari R, Ilmoniemi RJ, Knuutila J, Lounasmaa OV. Magnetoencephalography: theory, instrumentation, and application to noninvasive studies of the working human brain. Rev Mod Phys 1993;65:413–97.
[3] Knake S, Grant PE, Stufflebeam SM, Wald LL, Shiraishi H, Rosenow F, et al. Aids to telemetry in the presurgical evaluation of epilepsy patients: MRI, MEG and other non-invasive imaging techniques. Suppl Clin Neurophysiol 2004;57:494–502.
[4] Grondin R, Chuang S, Otsubo H, Holowka S, Snead 3rd OC, Raybaud C, et al. The role of magnetoencephalography in pediatric epilepsy surgery. Childs Nerv Syst 2006;22:779–85.
[5] Cappell J, Schevon C, Emerson RG. Magnetoencephalography in epilepsy: tailoring interpretation and making inferences. Curr Neurol Neurosci Rep 2006;6:327–31.
[6] Mäkelä JP, Forss N, Jääskeläinen J, Kirveskari E, Korvenoja A, Paetau R. Magnetoencephalography in neurosurgery. Neurosurgery 2006;59:493–510, [discussion 510–11].
[7] Shibasaki H, Ikeda A, Nagamine T. Use of magnetoencephalography in the presurgical evaluation of epilepsy patients. Clin Neurophysiol 2007;118:1438–48.
[8] Rampp S, Stefan H. Magnetoencephalography in presurgical epilepsy diagnosis. Expert Rev Med Devices 2007;4:335–47.
[9] Schwartz ES, Dlugos DJ, Storm PB, Dell J, Magee R, Flynn TP, et al. Magnetoencephalography for pediatric epilepsy: how we do it. AJNR Am J Neuroradiol 2008;29:832–7.
[10] Nakasato N, Levesque MF, Barth DS, Baumgartner C, Rogers RL, Sutherling WW, et al. Comparisons of MEG, EEG, and ECoG source localization in neocortical partial epilepsy in humans. Electroencephalogr Clin Neurophysiol 1994;91:171–8.

[11] Sutherling WW, Crandall PH, Engel Jr J, Darcey TM, Cahan LD, Barth DS. The magnetic field of complex partial seizure agrees with intracranial localizations. Ann Neurol 1987;21: 548–58.
[12] Shiraishi H, Watanabe Y, Watanabe M, Inoue Y, Fujiwara T, Yagi K. Interictal and ictal magnetoencephalographic study in patients with medial frontal lobe epilepsy. Epilepsia 2001;42:875–82.
[13] Oishi M, Kameyama S, Masuda H, Tohyama J, Kanazawa O, Sasagawa M, et al. Single and multiple clusters of magnetoencephalographic dipoles in neocortical epilepsy: Significance in characterizing the epileptogenic zone. Epilepsia 2006;47:355–64.
[14] Otsubo H, Ochi A, Elliott I, Chuang SH, Rutka JT, Jay V, et al. MEG predicts epileptic zone in lesional extrahippocampal epilepsy: 12 pediatric surgery cases. Epilepsia 2001;42:1523–30.
[15] Oppenheim A, Schafer RW, Buck JR. Discrete-time signal processing. New Jersey: Prentice Hall; 1999.
[16] Sueda K, Takeuchi F, Shiraishi H, Nakane S, Asahina N, Kohsaka S, et al. MEG time–frequency analyses for pre- and post-surgical evaluation of patients with epileptic rhythmic fast activity. Epilepsy Res 2010;88:100–7.
[17] Yagyu K, Takeuchi F, Shiraishi H, Nakane S, Sueda K, Asahina N, et al. The applications of time–frequency analyses to ictal magnetoencephalography in neocortical epilepsy. Epilepsy Res 2010;90:199–206.
[18] Oishi A, Tobimatsu S, Ochi H, Ohyagi Y, Kubota T, Taniwaki T, et al. Paradoxical lateralization of parasagittal spikes revealed by back averaging of EEG and MEG in a case with epilepsia partialis continua. J Neurol Sci 2002;193:151–5.
[19] Westmoreland BF. The EEG finding in extratemporal seizures. Epilepsia 1998;39(Suppl. 4):S1–8.
[20] Verma A, Radtke R. EEG of partial seizures. J Clin Neurophysiol 2006;23:333–9.

Epilepsia, 52(12):e204–e206, 2011
doi: 10.1111/j.1528-1167.2011.03299.x

BRIEF COMMUNICATION

Direct correlation between the facial nerve nucleus and hemifacial seizures associated with a gangliocytoma of the floor of the fourth ventricle: A case report

***Kazuyori Yagyu, *Keitaro Sueda, *Hideaki Shiraishi, *Naoko Asahina, †Kotaro Sakurai, *Shinobu Kohsaka, ‡Yutaka Sawamura, and *Shinji Saitoh**

Departments of *Pediatrics, †Psychiatry and ‡Neurosurgery, Hokkaido University Graduate School of Medicine, Sapporo, Japan

Summary

A dysplastic neuronal lesion of the floor of the fourth ventricle (DNFFV) causes hemifacial seizures (HFS) from early infancy. However, it is still controversial whether HFS is generated by the facial nerve nucleus or cerebellar cortex. In this study, we confirm a direct correlation between the rhythmic activities in the DNFFV and HFS using intraoperative electroencephalography (EEG) and electromyography (EMG) monitoring. Our results support the theory that a DNFFV provokes ipsilateral HFS via the facial nerve nucleus.

KEY WORDS: Facial nerve nucleus, Hemifacial seizure, Dysplastic neuronal lesion, Floor of the fourth ventricle.

There are several reports of hemifacial seizures (HFS) caused by dysplastic neuronal lesions of the floor of the fourth ventricle (DNFFV). Delalande et al. (2001) described theta or beta rhythmic activity in the DNFFV using a depth electrode inserted during surgery. However, there have been no reports elucidating a direct correlation between DNFFV and HFS or explaining the possible pathophysiology of a relationship between DNFFV and HFS. In this study, we sought to assess the pathophysiology of DNFFV and HFS by real-time monitoring of HFS during surgery.

Case Report

The patient was a 20-month-old boy who was born without perinatal problems. However, he had seizures with motion arrest and right eyelid contraction soon after birth. At 3 months of age, brain magnetic resonance imaging (MRI) demonstrated a mass lesion on the right side of the floor of the fourth ventricle, which showed isointensity to gray matter in both the T_1- and T_2-weighted images and was not enhanced by gadolinium injection. From 4 months of age, his seizures changed to intermittent closure of the right eye and right perioral contraction. Although the patient's psychomotor development was normal in infancy, he could not walk alone at 20 months. His seizures increased gradually and by 20 months of age were occurring every day at almost 20-s intervals while he was both awake and asleep.

He underwent tumor resection at 20 months of age. An MRI study obtained for preoperative evaluation revealed a mass lesion the same as at 3 months of age (Fig. 1A). Written informed consent was obtained for intraoperative monitoring before the operation. Needle electrodes were inserted into the right upper and lower eyelids and the right orbicular muscle of the mouth to detect the hemifacial seizures during surgery. A muscle relaxant was not used. Sheet electrodes with 20 contacts were used for evaluating cerebellar cortices, and a strip electrode with four contacts was used within the fourth ventricle.

During the surgery, although the sheet electrodes on the bilateral cerebellar cortices did not show any ictal findings related with eyelid twitching, the strip electrode on the tumor demonstrated rhythmic theta waves during eyelid twitching corresponding to electromyography (EMG) (Fig. 1B,C). At the moment of biopsy resection, aberrant EMG occurred with wild eyelid twitching, and then the patient's seizure disappeared soon after approximately half of the mass was resected during the biopsy. Subtotal removal was achieved finally and we confirmed no abnormal EMG indicating eyelid twitching or oral contraction and no rhythmic theta waves on the floor of the fourth ventricle. Pathology of the specimen showed a gangliocytoma.

Accepted September 4, 2011; Early View publication November 2, 2011.

Address correspondence to Shinji Saitoh, North 15, West 7, Kita-ku, Sapporo, Hokkaido 060-8638, Japan. E-mail: ss11@med.nagoya-cu.ac.jp